JOC The Journal of Organic Chemistry

Article

pubs.acs.org/joc

Nonplanar Monocyanines: *Meso*-Substituted Thiazole Orange with High Photostability and Their Synthetic Strategy as well as a Cell Association Study

Li Guan,[†] Anyang Li,[†] Yinyin Song,[†] Mengqi Yan,[†] Dengfeng Gao,[†] Xianghan Zhang,[‡] Bin Li,*[,§] and Lanying Wang*[,†]

[†]Key Laboratory of Synthetic and Natural Functional Molecule Chemistry, Ministry of Education, College of Chemistry and Materials Science, Northwest University, Xi'an 710127, People's Republic of China

[‡]School of Life Sciences and Technology, Xidian University, Xi'an 710071, People's Republic of China

[§]Key Laboratory of Resource Biology and Biotechnology in Western China, Ministry of Education, Northwest University, Xi'an 710069, People's Republic of China

Supporting Information

ABSTRACT: A convenient approach for the direct synthesis of *meso*-substituted thiazole orange (*meso*-TO) analogues has been unprecedentedly developed through the $AlCl_3$-catalyzed reaction of parent TO with benzyl alcohol derivatives. Single-crystal X-ray structures show that the prepared new *meso*-TO analogues are nonplanar, forming a sharp contrast to planar TO. The spectral properties show that nonplanar *meso*-TO analogues do not aggregate, existing in monomer form (M) in PBS buffer, and have little effect of solvatochromism in different solvents. In comparison with the parents, *meso*-TO analogues exhibit a large Stokes shift, excellent light fastness, and inertness to singlet oxygen. A cellular association study demonstrates that incorporation of a benzyl group at the *meso* position methine of parent TO can decrease the cytotoxicity, change staining area in cells, and emit long-wavelength fluorescence for an extended time, which are useful for the development of smarter TOs for imaging in biological science.

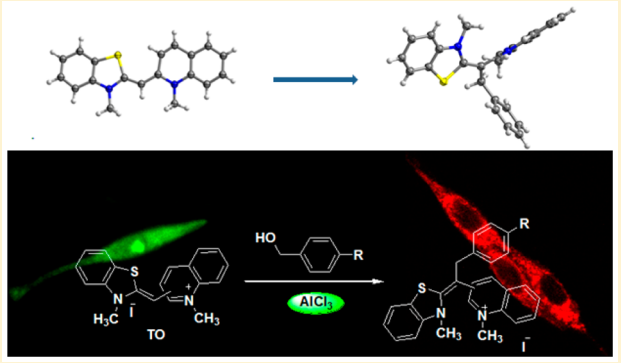

INTRODUCTION

Monocyanines are widely used in the biomedicine[1,2] and materials[3−5] fields due to their unique donor−π−acceptor (D−π−A) structure, straightforward synthesis,[6−9] tunable spectra, high extinction coefficient, and moderate to high fluorescence quantum yields after binding to nucleic acids.[10−13] However, problems such as their susceptibility to form nonfluorescent aggregates[14,15] and tendency to undergo photobleaching[16] also exist. To improve resistance to both aggregation and photobleaching, previous research was targeted to the de novo synthesis of photostabilized monocyanines from modified heterocycles. For example, Silva et al.[17] first introduced the electron-withdrawing group fluorine or trifluoromethyl to heterocycles and then synthesized a series of monocyanines from fluorinated heterocycles, and an investigation of their photophysical properties showed a reduction in aggregation and improvement in photostability. Shank et al.[18] introduced cyanomethylene to the 2-position of benzothiazole by quaternization and a malonic ester type reaction of 2-methylthiobenzothiazole and from the cyanomethylene-substituted benzothiazolium prepared a thiazole orange with cyano on the *meso* position methine, which showed inertness to visible light and singlet oxygen. The obvious disadvantage of such a approach is the multistep synthesis for each monocyanine. Here, we report a fast, facile, and effective direct synthesis method for generating new *meso*-substituted monocyanines with high resistance to both aggregation and photobleaching from more accessible parent monocyanines.

It is known that monocyanines can be easily synthesized from readily available and inexpensive reagents. Furthermore, their *meso* position methine belongs to the C-terminus of enamine, having nucleophilic reactivity, which can react with electrophile followed by loss of a proton to give *meso*-substituted monocyanines. We predict that they have considerable stability because stable *zaitsev alkene* is formed and steric hindrance is increased to make stacking unfavorable.

Thiazole orange (TO) constitutes an important subclass within the monocyanine family due to its applications in biological medicine,[19−21] and our previous efforts have been devoted to developing the synthesis and applications of

Received: April 24, 2016
Published: July 5, 2016

ACS Publications © 2016 American Chemical Society

DOI: 10.1021/acs.joc.6b00928
J. Org. Chem. 2016, 81, 6303−6313

Scheme 1. Reaction of 2TO and 1a[a]

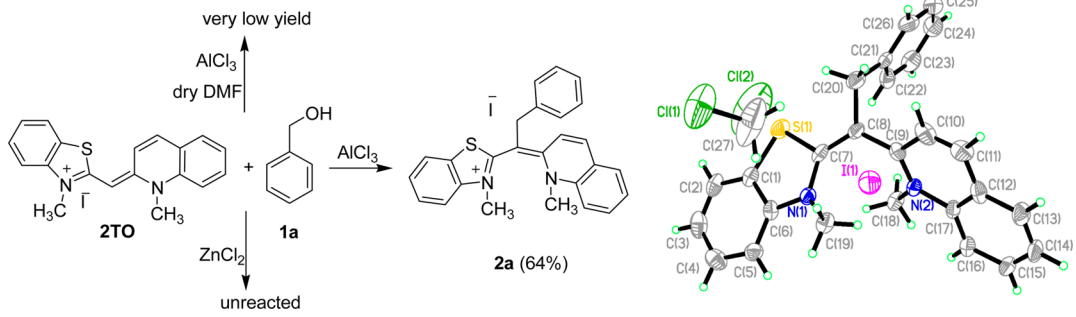

[a]The ellipsoid contour of **2a** is drawn at the 30% probability level.

monocyanines.[22,23] Moreover, benzyl alcohol (BnOH) derivatives are highly reactive and readily form electrophile benzyl carbocation under Lewis acid catalysis. Therefore, in this study we explored the reaction between parent TO and benzyl alcohol derivatives (Scheme 1 and Table 1) in the presence of Lewis acid to expand the direct synthesis method of valuable *meso*-substituted TO (*meso*-TO) analogues and investigated the spectral properties and photostability, as well as cytotoxicity and fluorescence images, of prepared new *meso*-TO analogues. Just as we expected, the designed direct synthesis method demonstrated several advantages including simple experimental procedures, mild reaction conditions, and good yields within a short time, and the new *meso*-TO analogues obtained showed a unique performance. To the best of our knowledge, this is the first report of the direct synthesis of *meso*-substituted monocyanines from the parent monocyanines.

Table 1. Optimal Conditions and Yields for the Synthesis of *meso*-TO Analogues[a]

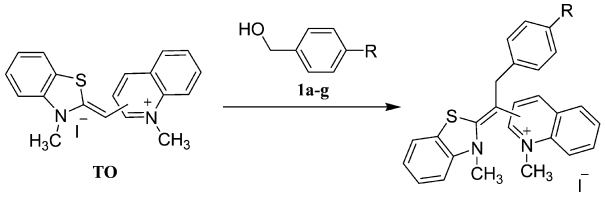

2TO: 2-Linked Quinoline nucleus
4TO: 4-Linked Quinoline nucleus
2a-g, 2-Linked Quinoline nucleus
3a-g, 4-Linked Quinoline nucleus

a: R=H; **b:** R=OH; **c:** R=OCH_3; **d:** R=CH_3; **e:** R=$CH(CH_3)_2$; **f:** R=Cl; **g:** R=NO_2

product	TO	R	solvent	temp (°C)	time	yield[b] (%)
2a	2TO	H		110	8 h	65
2b	2TO	OH	DMF	80	20 min	89
2c	2TO	OCH_3		80	2 h	83
2d	2TO	CH_3		110	6 h	69
2e	2TO	$CH(CH_3)_2$		110	6 h	66
2f	2TO	Cl		110	12 h	42
2g	2TO	NO_2		150	20 h	
3a	4TO	H		80	6 h	70
3b	4TO	OH	DMF	80	5 min	62
3c	4TO	OCH_3		80	0.5 h	81
3d	4TO	CH_3		80	6 h	74
3e	4TO	$CH(CH_3)_2$		80	6 h	55
3f	4TO	Cl		80	12 h	43
3g	4TO	NO_2		150	20 h	

[a]Reactions were performed in the presence of $AlCl_3$ (30 mol %). [b]Isolated yield after column purification.

RESULTS AND DISCUSSION

Synthesis of *meso*-TO Analogues. We first carried out the reaction between 2TO and BnOH (**1a**) (Scheme 1) using anhydrous $ZnCl_2$ as a catalyst in dichloromethane (DCM) under reflux, in dimethylformamide (DMF) at 40, 60, 80, 110, 130 °C, and reflux, or under solvent-free conditions at 60, 80, 110, 130, and 150 °C. Analysis showed no reaction between 2TO and **1a** using $ZnCl_2$ catalysis. Then the catalyst was changed to $AlCl_3$, and the reaction of 2TO with **1a** still did not take place in DCM under reflux, whereas slightly better results were obtained when the reaction temperature was increased to 110 °C in DMF. After that, trying to find appropriate conditions to achieve moderate to good yields of *meso*-Bn-2TO (**2a**), we observed that, using $AlCl_3$ (30 mol %) catalysis under solvent-free conditions, the reaction at 110 °C for 8 h gave **2a** in 64% yield, which was unambiguously determined on the basis of single-crystal X-ray diffraction analysis (Scheme 1). This constituted the first example of monocyanine chemistry based on *meso* position methine hydrocarbylation. To study the scope of this procedure, the reaction of 2TO or 4TO with different electrophiles was essayed (Table 1).

We examined the reactions of 2TO with various benzyl alcohol derivatives in the presence of $AlCl_3$ (30 mol %). Optimal results are shown in Table 1. Treatment of 2TO with *p*-CH_3BnOH (**1d**), *p*-$(CH_3)_2$CHBnOH (**1e**), or *p*-ClBnOH (**1f**) under solvent-free conditions at 110 °C for 6−12 h gave *meso*-*p*-CH_3Bn-2TO (**2d**; 69%), *meso*-*p*-$(CH_3)_2$CHBn-2TO (**2e**; 66%), and *meso*-*p*-ClBn-2TO (**2f**; 42%), respectively. When *p*-HOBnOH (**1b**) and *p*-CH_3OBnOH (**1c**) were used, the reactions proceeded efficiently at 80 °C for 20 min to 2 h, giving an 89% yield of *meso*-*p*-HOBn-2TO (**2b**) in DMF and an 83% yield of *meso*-*p*-CH_3OBn-2TO (**2c**) under solvent-free conditions. No reaction occurred at 110−150 °C when *p*-O_2NBnOH (**1g**) was used. Next, the reactions between 4TO and different benzyl alcohol derivatives were also essayed (Table 1). The reaction of 4TO with **1b** at 80 °C for 5 min in DMF gave the corresponding *meso*-*p*-HOBn-4TO (**3b**). When other benzyl alcohol derivatives such as **1a,c−f** were used, the corresponding products were also obtained at 80 °C for 0.5−12 h in moderate to good yields, while the reaction of 4TO with **1g** did not take place at high temperature (150 °C). Significantly, the presence of an electron-donating group such as a hydroxyl moiety on the benzyl benzene ring reduced the reaction temperature or time. In contrast, no reaction occurred

DOI: 10.1021/acs.joc.6b00928
J. Org. Chem. 2016, 81, 6303−6313

Scheme 2. Proposed Reaction Pathway for the Direct Synthesis of *meso*-TO Analogues

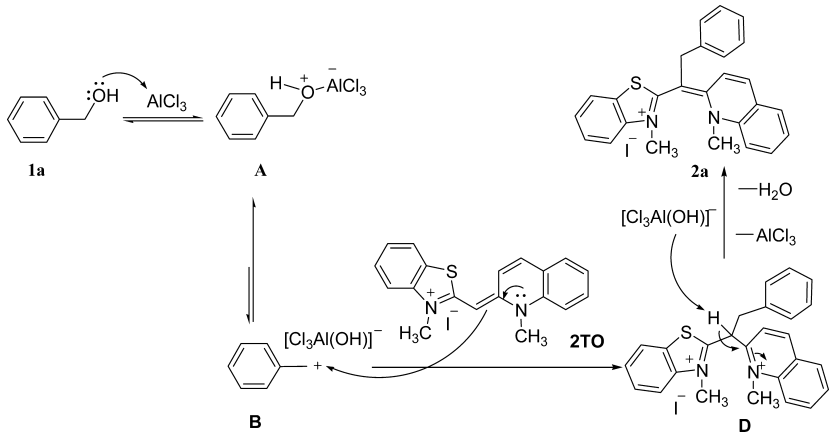

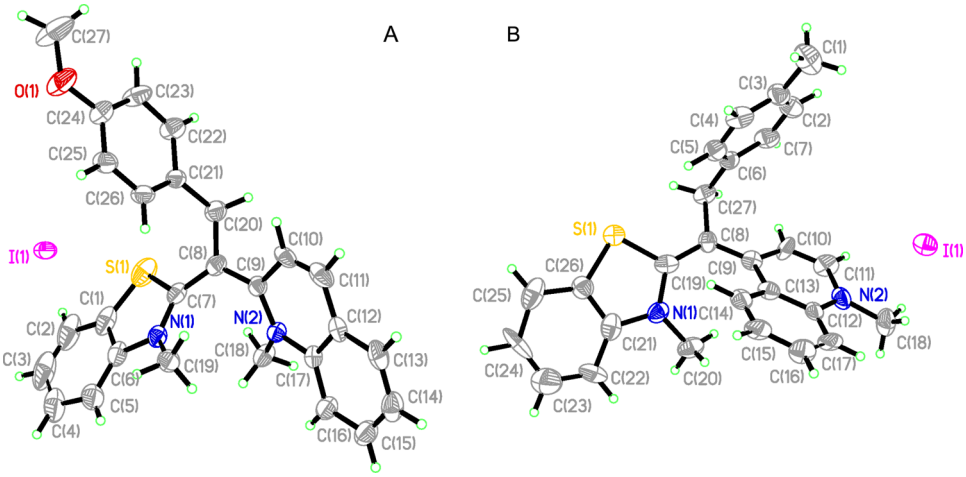

Figure 1. ORTEP views of the molecular structures of (A) **2c** and (B) **3d** with ellipsoids drawn at the 30% probability level.

when an electron-withdrawing group such as a nitro moiety was introduced onto the benzyl benzene ring. Moreover, the sequence of the reaction activity of benzyl alcohol derivatives with 2TO or 4TO was *p*-HOBnOH > *p*-CH_3OBnOH > *p*-CH_3BnOH ≈ *p*-$(CH_3)_2$CHBnOH > BnOH > *p*-ClBnOH > *p*-O_2NBnOH. These results suggested that benzyl carbocations might be involved as reactive intermediates, which was consistent with our original design. In short, the direct synthesis of *meso*-TO analogues from parent TO was convenient, and the yields were moderate to high. The purification could readily be carried out by silica gel column chromatography. We were very fortunate to verify the *meso*-TO analogues **2a,c**, and **3d** by NMR and single-crystal X-ray diffraction.

A proposed reaction pathway is shown in Scheme 2 (taking the reaction of 2TO and benzyl alcohol (**1a**) as an example). First, the reaction between **1a** and $AlCl_3$ gives the molecular complex **A** with a positive charge on oxygen and a negative charge on aluminum, and redistribution of electrons in this complex generates the benzyl carbocation **B**. Second, attack of **B** on the *meso* position methine of 2TO results in the formation of hydrocarbylation intermediate **D**. Finally, proton transfer from **D** to $[Cl_3Al(OH)]^-$ forms H_2O, regenerates $AlCl_3$, and gives *meso*-TO **2a**. To give a deep insight into the features of species **A** and **B**, their potential energies including zero-point correction relative to the reactants were calculated on the basis of optimized geometries at the B3LYP/6-31+G* level. As a result, both **A** and **B** are thermally stable with stabilization energies of −110.4 and −43.5 kJ/mol, respectively. Since the difference in the stabilization energies of the two species is modest, and the sequence of the reaction activity of benzyl alcohol derivatives with 2TO or 4TO is *p*-HOBnOH > *p*-CH_3OBnOH > *p*-CH_3BnOH ≈ *p*-$(CH_3)_2$CHBnOH > BnOH > *p*-ClBnOH > *p*-O_2NBnOH, there is an equilibrium between species **A** and **B**, which favors species **A**.

X-ray Structures. Crystals suitable for X-ray analysis were obtained by slow evaporation of a solution of TO or *meso*-TO. Compounds crystallized in the triclinic space group $P\bar{1}$ for 2TO and **2a,c**, in the orthorhombic space group $Pna2_1$ for 4TO, and in the monoclinic space group $P2_1/n$ for **3d** (Figure 1, Figures S1 and S2 in the Supporting Information, and Scheme 1). Analysis shows that in 2TO and 4TO two heterocyclic rings and central methine are almost coplanar with dihedral angles of 8.26 and 0°, respectively. In addition, the new *meso*-TO analogues are severely twisted out of plane by benzyl on *meso*-methine with dihedral angles of 50.51, 47.43, and 53.80° for **2a,c** and **3d**, respectively. The average distances between *meso*-C and methene-C of **2a,c** and **3d** are 1.52, 1.49, and 1.50 Å, respectively, which is basically intermediate between typical C−C single (1.54 Å) and C=C double bonds (1.34 Å), implying the occurrence of $\sigma-\pi$ hyperconjugation between methene on benzyl and D−π−A.

The crystal packing of 2TO and 4TO is given in Figure S3 in the Supporting Information. It is found that 2TO and 4TO

DOI: 10.1021/acs.joc.6b00928
J. Org. Chem. 2016, 81, 6303−6313

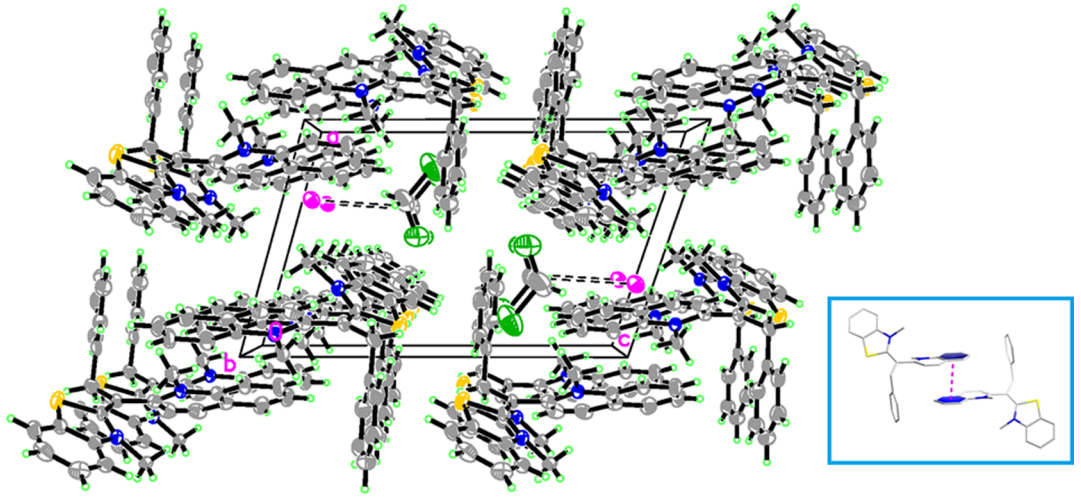

Figure 2. Crystal packing of **2a**.

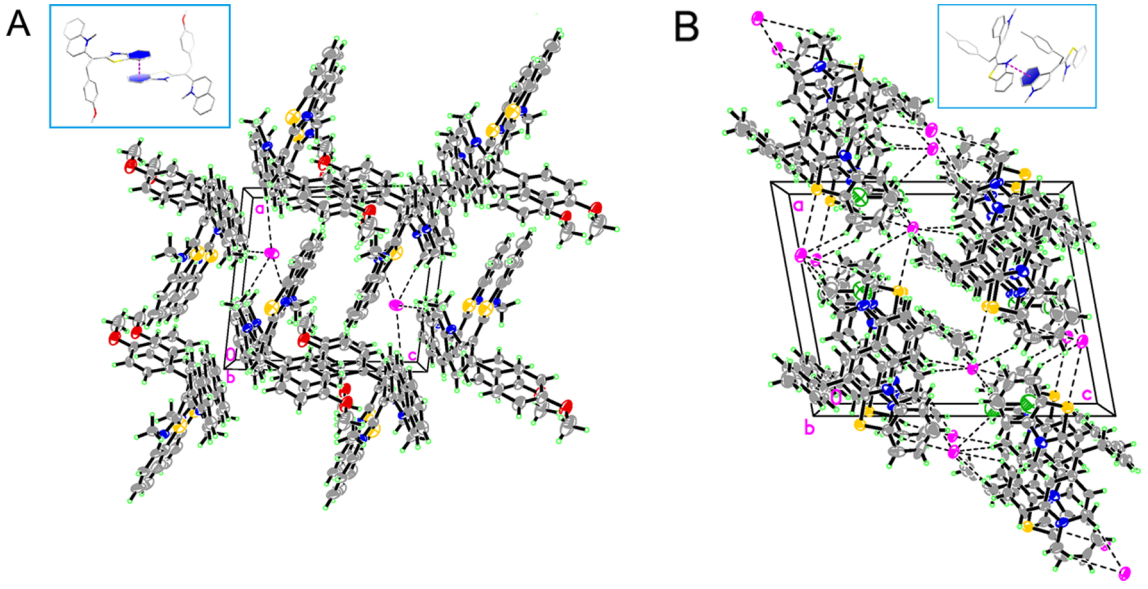

Figure 3. Crystal packing of (A) **2c** and (B) **3d**.

Table 2. Spectral Data of TO and *meso*-TO Analogues in Different Solvents

	MeOH		PBS buffer		90% glycerol			
dye	λ_{max} (nm)	$10^{-4}\varepsilon$ (L mol^{-1} cm^{-1})	λ_{max} (nm)	$10^{-4}\varepsilon$ (L mol^{-1} cm^{-1})	λ_{max} (nm)	$10^{-4}\varepsilon$ (L mol^{-1} cm^{-1})	λ_{em} (nm)[a]	Stokes shift (nm)
2TO	483	3.52	479	3.25	487	3.24	560	73
2a	520	1.91	518	1.61	526	1.88	607	81
2b	523	2.94	517	2.76	526	2.67	620	94
2c	522	1.30	520	1.21	526	1.33	621	95
2d	521	1.82	521	1.64	524	1.76	617	93
2e	521	2.35	521	2.06	528	2.55	613	85
2f	519	1.97	517	1.76	522	1.91	618	96
4TO	502	6.36	500	3.73	507	6.71	552	45
3a	554	1.91	555	1.56	559	2.20	640	81
3b	556	2.84	556	2.25	560	2.50	640	80
3c	556	3.03	553	2.21	559	3.30	637	78
3d	555	2.74	552	1.85	555	2.50	637	82
3e	554	1.72	554	1.15	558	1.60	639	81
3f	554	1.78	552	1.35	556	1.90	643	87

[a]Excited at the maximum absorption wavelengths.

DOI: 10.1021/acs.joc.6b00928
J. Org. Chem. 2016, 81, 6303−6313

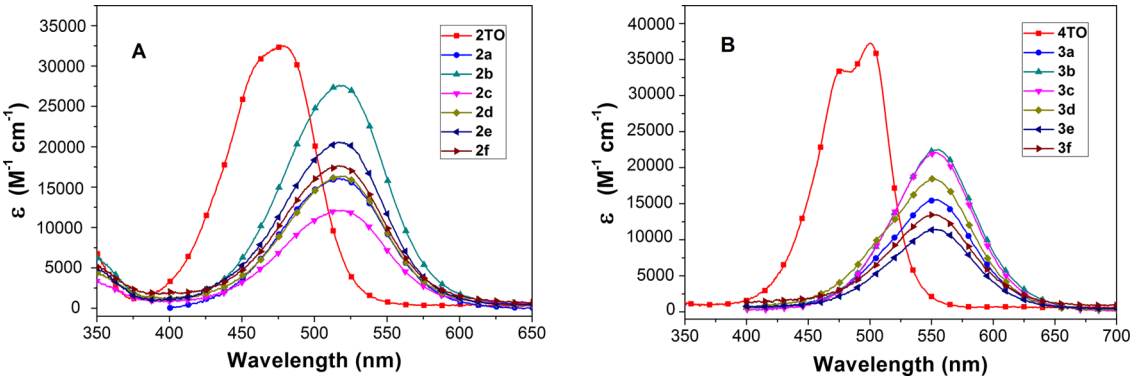

Figure 4. UV−vis spectra recorded for TO or *meso*-TO (10 μM) in PBS buffer: (A) 2TO and **2a**−**f**; (B) 4TO and **3a**−**f**.

molecules are all stacked via $\pi-\pi$ interactions with face-to-face distances of 3.68 and 3.61 Å, respectively. The adjacent molecules are arranged in a head-to-tail orientation by intermolecular hydrogen bonds C(10)−H(10)···S(1) (2.51 Å) for 2TO and C(11)−H(11)···S(1) (2.39 Å) for 4TO. In the crystal packing of **2a** (Figure 2), the quinoline ring planes are parallel to each other, and there are $\pi-\pi$ stacking interactions with face-to-face distances of 3.76 Å. Interestingly, the adjacent molecules are arranged in a head-to-tail fashion on the basis of intermolecular hydrogen bonds, C(20)−H(20A)···S(1) (2.57 Å), C(18)−H(18C)···N(1) (2.27 Å), and C(19)−H(19C)···N(2) (2.36 Å), which stabilize the molecular packing. Identically, for **2c** (Figure 3), the benzothiazole ring planes are parallel to each other having $\pi-\pi$ stacking interactions with face-to-face distances of 4.29 Å, and the adjacent molecules are arranged in a head-to-tail fashion on the basis of an intermolecular hydrogen bond C(20)−H(20A)···S(1) (2.65 Å). In the packing of **3d** (Figure 3), the quinoline ring and benzothiazole ring are stacked through $\pi-\pi$ interactions with face-to-face distances of 4.07 Å, and the adjacent molecules are arranged by a C(27)−H(27A)···S(1) (2.39 Å) intermolecular hydrogen bond in a head-to-tail orientation.

Photophysical Characterization. The spectroscopic properties of *meso*-TO analogues **2a**−**3f** and parent TO were determined in methanol, PBS buffer, and 90% glycerol−water. The relevant data are summarized in Table 2, and their absorption spectra in PBS buffer are shown in Figure 4. It could be observed that **2a**−**f** and **3a**−**f** did not aggregate, existing in monomer form (M) in PBS buffer. The absorption maxima (λ_{max}) were located in the range of 517−528 nm for **2a**−**f** and 554−560 nm for **3a**−**f** in different solvents, showing little effect of the substituent on benzyl and solvatochromism. In comparison with the corresponding parent TO, the λ_{max} values of **2a**−**f** and **3a**−**f** were found to be red-shifted 39 ± 3 and 52 ± 4 nm in PBS buffer, respectively, and their curve shapes also changed. That is, the spectra of **2a**−**3f** showed a single peak, whereas the spectra of 2TO and 4TO had an additional peak at shorter wavelength, which was characteristic of their assembly into H-aggregates.[24,25] This could be attributed to the fact that the $\sigma-\pi$ hyperconjugation between methene on benzyl and D−π−A structure made the conjugated system larger (see X-ray Structures), causing the red shift of λ_{max}, and steric hindrance caused by *meso*-benzyl made molecule stacking unfavorable, leading to the species existing in the M form instead of aggregates.

Since TO and *meso*-TO analogues did not fluoresce in a nonviscous solvent (methanol or aqueous solution), we investigated their emission spectra in a viscous solvent (90% glycerol−water) (Table 2). It could be observed that the emission maxima (λ_{em}) were less affected by a substituent on benzyl. In comparison with the corresponding parent TO, the λ_{em} values of **2a**−**f** and **3a**−**f** were red-shifted 54 ± 7 and 88 ± 3 nm, respectively, while they were not as bright as the parent TO (Figure 5). In addition, the Stokes shift of *meso*-TO was

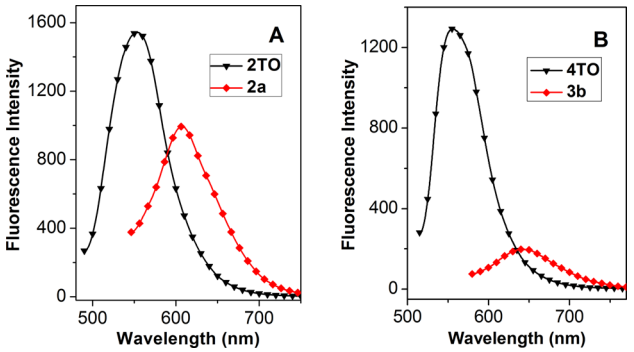

Figure 5. Fluorescence spectra recorded for 1 μM TO or 5 μM *meso*-TO in 90% glycerol−water: (A) 2TO and **2a**; (B) 4TO and **3b**. Samples were excited at 480 nm.

larger than that of the corresponding parent TO, such as 73 nm for 2TO and 95 nm for **2c** and 45 nm for 4TO and 82 nm for **3d**. This was attributed to the fact that the benzyl group interrupted the plane of the molecules and thus decreased the rigidity of the molecular structure, increasing the Stokes shift.[26,27]

Photostability. High photostability of cyanine dyes is one of the most important characters for practical applications. Their poor photostability is caused by singlet oxygen ($^1O_2$) that oxidizes excited dye molecules under light irradiation.[28,29] In view of this, we investigated the photostability of *meso*-TO analogues **2a**−**3f** and parent TO in PBS buffer by irradiating samples with a 500 W iodine−tungsten (I/W) lamp for 1 h and evaluating their absorption spectra. As shown in Figure 6, the *meso*-TO analogues showed good to excellent photostability. After irradiatinon for 60 min, *meso*-2TOs **2a**−**f** and *meso*-4TOs **3a**−**f** exhibited less than 5% and 17% photofading, respectively, while 2TO and 4TO showed more than 15% and 50% photofading, respectively.

We also performed thermal bleaching studies on TO and *meso*-TO analogues in the presence of sodium molybdate, which reacted with hydrogen peroxide under alkaline conditions to generate $^1O_2$ via a thermal process.[30,31] As

DOI: 10.1021/acs.joc.6b00928
J. Org. Chem. 2016, 81, 6303−6313

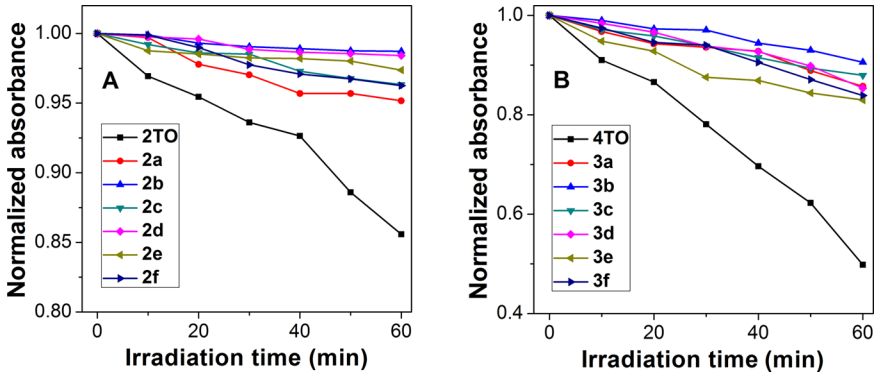

Figure 6. Comparison of photofading: (A) 2TO and *meso*-2TOs; (B) 4TO and *meso*-4TOs.

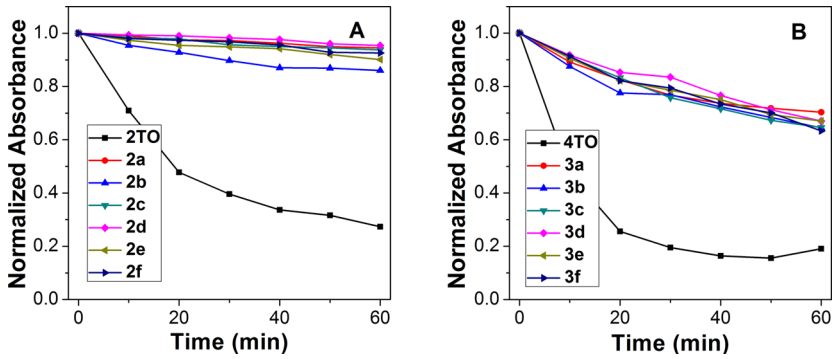

Figure 7. Time course of bleaching: (A) 2TO and *meso*-2TOs; (B) 4TO and *meso*-4TOs. Reactions were run in water with [dye] = 10 μM and pH 9, [Na_2MoO_4] = 50 mM, [H_2O_2] = 9.8 mM.

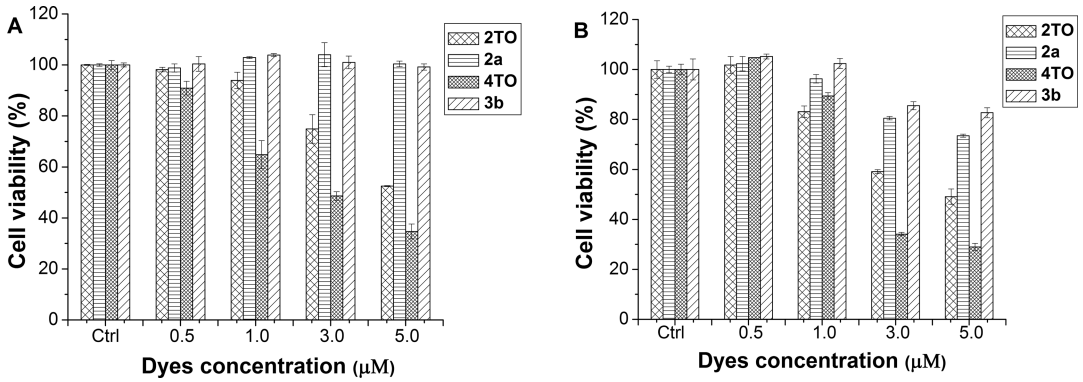

Figure 8. Cell viability of (A) RCF cells and (B) MCF-7 cells incubated with different concentrations of dyes for 24 h. Data represent the means ± SD of three independent experiments.

shown in Figure 7, the *meso*-TO analogues underwent bleaching much more slowly, whereas the parent TO was seriously destroyed by singlet oxygen. After 60 min continuous reaction, *meso*-2TOs **2a**–**f** and *meso*-4TOs **3a**–**f** showed 6%–15% and 30%–37% fading, respectively, while 2TO and 4TO sharply bleached by 73% and 81%, respectively. **2d** showed the best inertness to singlet oxygen with only 5% fading. From the above, incorporating a benzyl group at the *meso* position methine of parent TO reduced the reactivity of the D–π–A structure toward singlet oxygen and exhibited superior stability. The reason for their high stability might be that the hydrocarbylation of the *meso* position methine of parent TO formed stable *zaitsev alkene* and sterically hindered attack by singlet oxygen or other oxidation species. Moreover, the σ–π hyperconjugation between methene on benzyl and the D–π–A structure enlarged the conjugated system and made the *meso*-TO more stable. In order to further understand this point, the atomic charges of relevant atoms of 2TO, **2a**, 4TO, and **3d** were evaluated using natural bond orbital (NBO) analysis[32] at the B3LYP/6-31G* level. The NBO charges on the *meso* position carbons of 2TO, 4TO, **2a**, and **3d** were −0.420, −0.362, −0.203, and −0.170, respectively, which suggested that the electronic density of the *meso* position carbon in 2TO and 4TO was much larger than that in **2a** and **3d**. The lower electronic density of **2a** and **3d** made them hard to oxidize and gave them better stability.

Cytotoxicity. Low cytotoxicity is a stringent requirement for biomedical applications. Therefore, an MTT assay was performed to evaluate the cell toxicity of the selected *meso*-TO (**2a**, **3b**) and TO (2TO, 4TO). Rat cardiac fibroblasts (RCF) cells and human breast adenocarcinoma (MCF-7) cells were incubated with **2a**, **3b**, 2TO, or 4TO at different concentrations

DOI: 10.1021/acs.joc.6b00928
J. Org. Chem. 2016, 81, 6303–6313

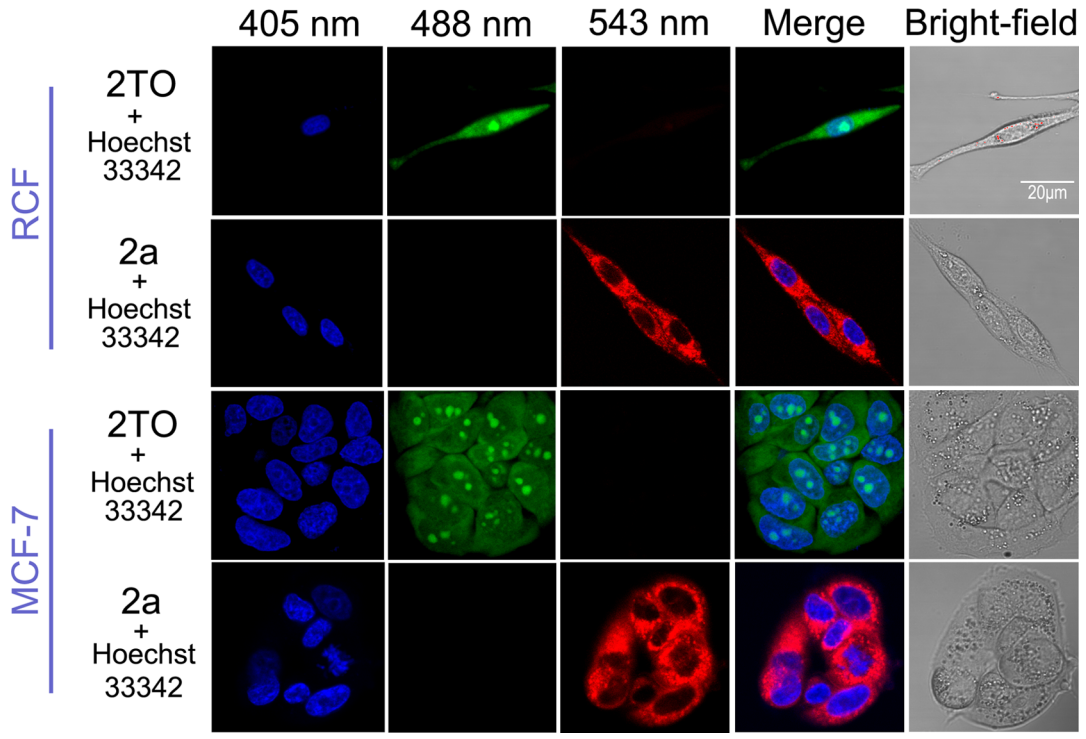

Figure 9. Confocal images of living cells with Hoechst 33342 (1 μM, excited at 405 nm), 2TO (1 μM, excited at 488 nm), and **2a** (3 μM, excited at 543 nm). The merge image is a overlay fluorescence from three channels.

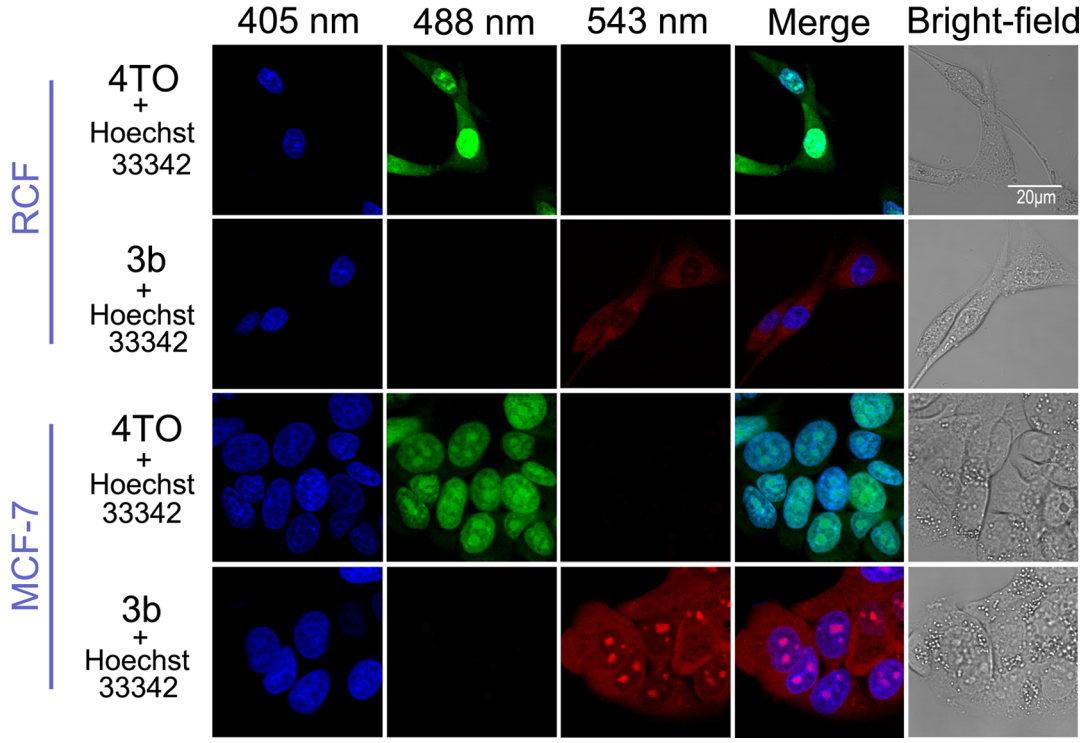

Figure 10. Fluorescence images of living cells with Hoechst 33342 (1 μM, excited at 405 nm), 4TO (1 μM, excited at 488 nm), and **3b** (3 μM, excited at 543 nm). The merge image is a overlay fluorescence from three channels.

for 24 h, and cell viabilities were measured. As shown in Figure 8, after incubation with **2a** or **3b** for 24 h, the cell viability at the maximum tested concentration of 5×10^{-6} M was close to 100% for RCF cells and more than 78% for MCF-7 cells. However, under the same conditions the cell viability was about 50% in the case of 2TO and about 30% in the case of 4TO for RCF and MCF-7 cells. The results indicated that **2a** and **3b** exhibited no cytotoxic effects for RCF cells and low cytotoxic effects for MCF-7 cells, and 2TO and 4TO exhibited high cytotoxic effects for RCF and MCF-7 cells. Therefore, incorporation of a benzyl group at the *meso* position methine of parent TO could reduce cytotoxic effects on cells.

DOI: 10.1021/acs.joc.6b00928
J. Org. Chem. 2016, 81, 6303−6313

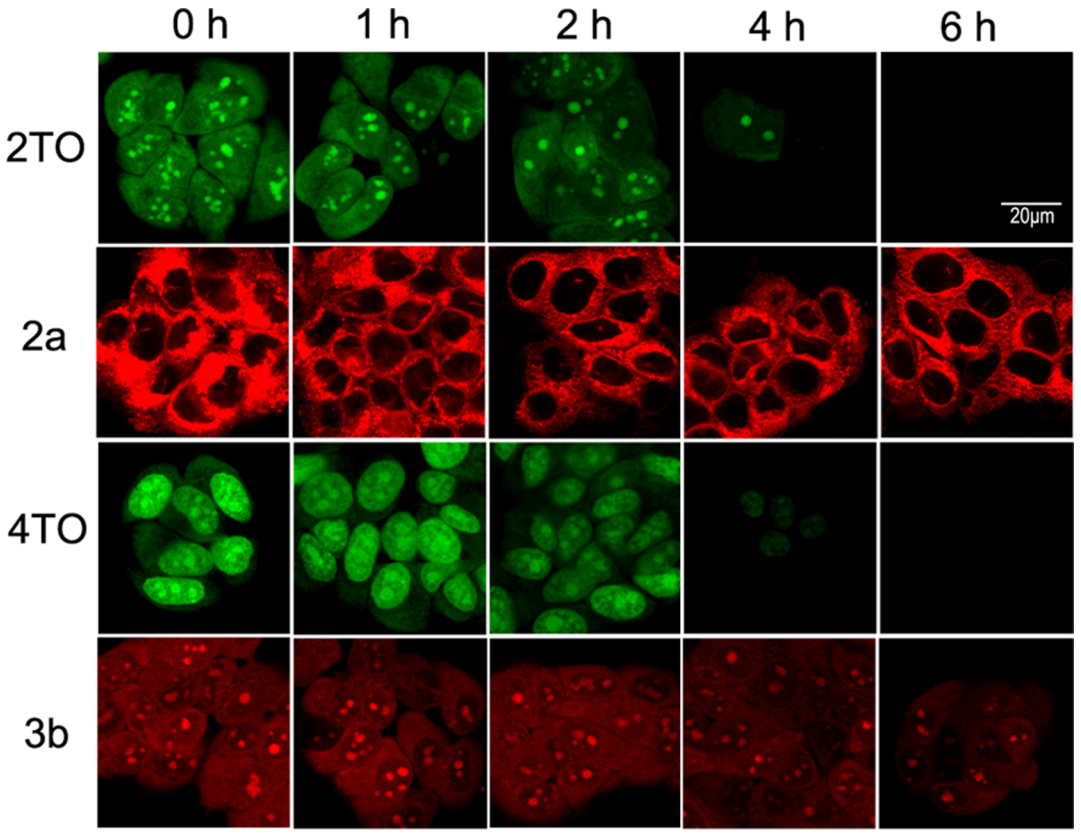

Figure 11. Photostability demonstration: the imaging of MCF-7 cells with 2TO, 4TO, **2a**, or **3b** in the range of 0−6 h.

Cell Staining and Fluorescence Imaging. *meso*-TOs (**2a**, **3b**) were subjected to cell imaging experiments and compared with 2TO and 4TO. To ensure the localization of TO and *meso*-TO, costaining assays were conducted using the commercially available cell nuclei marker dye Hoechst 33342. We imaged RCF and MCF-7 cells stained with 1−3 μM *meso*-TO, TO, or Hoechst 33342 at three different excitation wavelengths: 405, 488, and 543 nm. As shown in Figure 9, Hoechst 33342 stained nuclei and gave blue fluorescence upon excitation at 405 nm and 2TO stained both nuclei and cytoplasm and gave green fluorescence upon excitation at 488 nm, whereas **2a** could be accumulated in cells and mainly distributed in the cytoplasm, giving red fluorescence at 543 nm excitation. In addition, in cell imaging of 4TO and **3b** (Figure 10), the green channel clearly revealed that cells successfully uptake 4TO, and the fluorescence located in cell nuclei was brighter than that in cell cytoplasm. The fluorescence signals produced by **3b** were distributed in cell nuclei and cytoplasm in the red channel. The results of cell imaging demonstrated that incorporating a benzyl group at the *meso* position methine of parent TO could change staining areas in cells and cause fluorescence at longer wavelength.

In biological studies, highly photostable fluorescent dyes are urgently needed for the long-term observation of living cells. Therefore, imaging of MCF-7 cells stained with TO or *meso*-TO over the range of 0−6 h was performed. As shown in Figure 11, the green fluorescence from cells stained with 2TO or 4TO gradually decreased with the prolonged time, and the fluorescence signals became visually undetectable after 4 h. In contrast, the red fluorescence from cells stained with **2a** or **3b** remained basically unchanged with time, and no obvious fading off was observed. Obviously, *meso*-TOs **2a** and **3b** have a great potential to be applied as fluorescent dyes for the long-term observation of living cells.

CONCLUSION

A strategy for the direct synthesis of new *meso*-TO analogues through the $AlCl_3$-catalyzed reaction of parent TO with benzyl alcohol derivatives has been developed, which demonstrates several advantages, including simple experimental procedures, mild reaction conditions, and good yields within a short time. A performance survey revealed that addition of a benzyl group to the *meso* position methine of parent TO led to no aggregation in PBS buffer, relatively long absorption and emission maxima, and high photostability. A cellular association study demonstrated that synthesized *meso*-TOs had no or low cytotoxic effects for RCF and MCF-7 cells and could be used for long-term imaging for living cell cytoplasm staining, which was useful for the development of smarter TO dyes for technological applications.

EXPERIMENTAL SECTION

General Method. Thiazole oranges 2TO and 4TO were synthesized by the reaction of 2-methylthiobenzothiazolium salts with 2- or 4-methylquinolinium salts according to the literature.[33] Common reagents or solvents were obtained from commercial sources and used without further purification. DMF was dried and distilled by standard procedures. Melting points were uncorrected. NMR measurements were recorded with a 400 MHz spectrometer for ^{1}H NMR and with a 100 MHz spectrometer for ^{13}C NMR. HRMS analysis was done using a QTOF mass spectrometer. Absorption and fluorescence spectra were recorded on a UV−vis spectrometer and a spectrofluorimeter at room temperature.

Photostability. The photostability tests were carried out in quartz cells in a light-tight box, where sample solutions (10 μM of the

DOI: 10.1021/acs.joc.6b00928
J. Org. Chem. 2016, 81, 6303−6313

respective dye in PBS buffer) were irradiated with a 500 W iodine–tungsten (I/W) lamp at room temperature. To eliminate the heat and absorbing short wavelength light, a cold trap (1 L solution of water in a 20 cm × 3 cm × 20 cm glass container) was set up between the cell and the lamp, with a distance of 350 mm. An absorbance spectrum was scanned at 10 min intervals over a total of 1 h. The data were normalized to the highest value obtained for each sample.

Singlet Oxygen Reactivity.[18] Bleaching experiments were carried out in the presence of 50 mM sodium molybdate and 9.8 mM hydrogen peroxide containing 10 μM of dye. Hydrogen peroxide solution (30%) was added to PBS buffer solution (pH 9.0) to give a final concentration of 9.8 mM. The absorbance spectra of the dye solution containing hydrogen peroxide in the buffer solution were recorded, and then Na_2MoO_4 was added to the dye solution, which was scanned by a UV–vis spectrometer at 10 min intervals over a total of 1 h. The data were normalized to the highest value obtained for each sample.

Cell Culture. RCF cells and MCF-7 cells were all cultured in Dulbecco's Modified Eagle's Medium (DMEM) supplemented with 10% of fetal bovine serum (FBS, Gibco), 100 IU/mL of penicillin and 100 μg/mL of streptomycin at 37 °C in 95% humidified air and 5% CO_2.

Confocal Imaging. RCF cells and MCF-7 cells were seeded in 35 mm glass bottom dishes at a density of 1×10^5 cells/mL in complete medium, respectively. After 24 h, the cells were first stained with TO (1 μM) or *meso*-TO (3 μM) for 45 min and washed three times with PBS. Then the cells were incubated with Hoechst 33342 (1 μM) for 10 min and washed three times with PBS. After replacement of the medium, the cells were imaged using an Olympus FV1000 confocal fluorescence microscope with an 80× objective lens. The fluorescence images were acquired in the wavelength ranges of 425–475, 505–550, and 603–678 nm, respectively, using an argon laser at excitation wavelengths of 405, 488, and 543 nm, respectively. Confocal images were analyzed using an FV10-ASW 3.0 Viewer.

MTT Assay for Cell Cytotoxicity. Toxicities of TO or *meso*-TO toward RCF cells and MCF-7 cells were assessed by MTT assays for cell viability.[34] The cells were seeded at a density of 1×10^5 cells/mL in 96-well plates. After 24 h for attachment, the cells were treated with dye (2TO, **2a**, 4TO, or **3b**) at serial concentrations of 0.5, 1, 3, and 5 μM for 24 h. Then the medium was removed and the cells were washed with PBS. MTT solution (100 μL of 0.5 mg/mL in Opti-MEM) was added to each well, and the cells were further incubated for 4 h. After the supernatant was removed, blue MTT formazan precipitate was dissolved in 100 μL of DMSO. The plate was shaken for 10 min, and the absorbance was measured at 490 nm using an ELISA plate reader. All MTT assays were performed three times in duplicate.

Photobleaching in Cell Imaging. Assays were conducted in glass bottom dishes. After MCF-7 cells adhered to the bottom of the dish, 1 μM TO and 3 μM *meso*-TO (**2a** or **3b**) were added to individual cell culture dishes, respectively. Following 30 min incubation with TO or *meso*-TO, the cells were washed three times with medium. Then new medium was added and photobleaching images were taken on a fluorescence microscope. Image processing was performed using an FV10-ASW 3.0 Viewer.

General Procedure A for the Preparation of *meso*-TO Analogues 2a–3f. A mixture of 0.5 mmol of 2TO or 4TO, 2.5 mmol of benzyl alcohol derivative, and 0.15 mmol of $AlCl_3$ in 3 mL of anhydrous DMF was subjected to heat at the appropriate temperature. The progress of the reaction was monitored by TLC. After the reaction was completed, ice water was added to quench the reaction. The resulting reaction mixture was extracted with DCM, and the organic layer was washed with brine, dried with $MgSO_4$, filtered, and concentrated under reduced pressure to give the crude product, which was submitted to flash chromatography (silica gel; eluent methanol/dichloromethane 1/50 v/v).

General Procedure B for the Preparation of *meso*-TO Analogues 2a–3f. A mixture of 0.5 mmol of 2TO or 4TO, a suitable amount of benzyl alcohol derivative, and 0.15 mmol of $AlCl_3$ was subjected to heat at the appropriate temperature under solvent-free conditions. The progress of the reaction was monitored by TLC. After the reaction was completed, ice water was added to quench the reaction. The resulting reaction mixture was extracted with DCM, and the organic layer was washed with brine, dried with $MgSO_4$, filtered, and concentrated under reduced pressure to give the crude product, which was submitted to flash chromatography (silica gel; eluent methanol/dichloromethane 1/100 or 1/50 v/v).

*3-Methyl-2-[(1-methyl-2(1H)-quinolinylidene)benzylmethyl]-benzothiazolium Iodide (**2a**).* According to general procedure B, a mixture of 0.5 mmol of 2TO, 2 mL of benzyl alcohol (**1a**), and 0.15 mmol of $AlCl_3$ was reacted at 110 °C for 8 h under solvent-free conditions. Flash chromatography (methanol/dichloromethane, 1/100 v/v) afforded **2a** as a dark red solid (170 mg, 65%). Mp: 155–156 °C. ^{1}H NMR (400 MHz, DMSO-d_6): δ 8.48 (d, J = 9.2 Hz, 1H), 8.11 (t, J = 7.6 Hz, 2H), 7.99 (t, J = 8.4 Hz, 1H), 7.89 (d, J = 8.0 Hz, 1H), 7.81 (d, J = 9.2 Hz, 1H), 7.73 (t, J = 7.6 Hz, 1H), 7.54 (d, J = 3.6 Hz, 2H), 7.27–7.37 (m, 5H), 7.21–7.18 (m, 1H), 4.22 (s, 2H), 3.96 (s, 3H), 3.24 (s, 3H). ^{13}C NMR (100 MHz, DMSO-d_6): δ 164.1, 158.9, 143.6, 140.4, 140.0, 138.9, 133.9, 129.6, 129.2, 128.2, 128.1, 127.6, 127.1, 126.2, 125.8, 125.5, 124.8, 122.8, 119.2, 114.0, 93.1, 43.2, 41.6. HRMS (ESI-TOF) m/z: $[M - I]^+$ calculated for $C_{26}H_{23}N_2S^+$ 395.1576, found 395.1583.

*3-Methyl-2-[(1-methyl-2(1H)-quinolinylidene)-p-hydroxybenzyl-methyl]benzothiazolium Iodide (**2b**).* According to general procedure A, a mixture of 0.5 mmol of 2TO, 2.5 mmol of *p*-hydroxybenzyl alcohol (**1b**), and 0.15 mmol of $AlCl_3$ in 3 mL of anhydrous DMF was reacted at 80 °C for 20 min. Flash chromatography (methanol/dichloromethane, 1/50 v/v) afforded **2b** as a dark red solid (239 mg, 89%). Mp: 231–232 °C. ^{1}H NMR (400 MHz, DMSO-d_6): δ 9.29 (s, 1H), 8.47 (d, J = 9.1 Hz, 1H), 8.10 (t, J = 8.4 Hz, 2H), 7.99 (t, J = 8.4 Hz, 1H), 7.89 (d, J = 7.2 Hz, 1H), 7.79 (d, J = 9.1 Hz, 1H), 7.73 (t, J = 7.2 Hz, 1H), 7.53 (d, J = 3.6 Hz, 2H), 7.37–7.32 (m, 1H), 7.08 (d, J = 8.4 Hz, 2H), 6.66 (d, J = 8.4 Hz, 2H), 4.09 (s, 2H), 3.94 (s, 3H), 3.20 (s, 3H). ^{13}C NMR (100 MHz, DMSO-d_6): δ 163.9, 158.9, 156.5, 143.5, 140.4, 139.8, 133.8, 129.6, 129.2, 128.7, 128.0, 127.5, 126.1, 125.9, 125.6, 124.8, 122.8, 119.2, 115.9, 114.0, 94.0, 43.1, 41.0. HRMS (ESI-TOF) m/z: $[M - I]^+$ calculated for $C_{26}H_{23}N_2OS^+$ 411.1526, found 411.1538.

*3-Methyl-2-[(1-methyl-2(1H)-quinolinylidene)-p-methoxy-benzylmethyl]benzothiazolium Iodide (**2c**).* According to general procedure B, a mixture of 0.5 mmol of 2TO, 2 mL of *p*-methoxybenzyl alcohol (**1c**), and 0.15 mmol of $AlCl_3$ was reacted at 80 °C for 2 h under solvent-free conditions. Flash chromatography (methanol/dichloromethane, 1/100 v/v) afforded **2c** as a dark red solid (229 mg, 83%). Mp: 132–133 °C. ^{1}H NMR (400 MHz, DMSO-d_6): δ 8.47 (d, J = 8.8 Hz, 1H), 8.11 (t, J = 8.8 Hz, 2H), 7.99 (t, J = 8.4 Hz, 1H), 7.89 (d, J = 7.6 Hz, 1H), 7.80 (d, J = 8.8 Hz, 1H), 7.73 (t, J = 7.6 Hz, 1H), 7.53 (d, J = 4.0 Hz, 2H), 7.37–7.34 (m, 1H), 7.21 (d, J = 8.4 Hz, 2H), 6.84 (d, J = 8.8 Hz, 2H), 4.14 (s, 2H), 3.95 (s, 3H), 3.69 (s, 3H), 3.21 (s, 3H). ^{13}C NMR (100 MHz, DMSO-d_6): δ 164.0, 158.9, 158.4, 143.6, 140.4, 139.9, 133.8, 130.5, 129.6, 129.3, 128.0, 127.6, 126.2, 125.8, 125.5, 124.8, 122.8, 119.2, 114.6, 114.0, 93.7, 55.5, 43.2, 40.9. HRMS (ESI-TOF) m/z: $[M - I]^+$ calculated for $C_{27}H_{25}N_2OS^+$ 425.1682, found 425.1688.

*3-Methyl-2-[(1-methyl-2(1H)-quinolinylidene)-p-methyl-benzylmethyl]benzothiazolium Iodide (**2d**).* According to general procedure B, a mixture of 0.5 mmol of 2TO, 10.0 mmol of *p*-methylbenzyl alcohol (**1d**), and 0.15 mmol of $AlCl_3$ was reacted at 110 °C for 6 h under solvent-free conditions. Flash chromatography (methanol/dichloromethane, 1/100 v/v) afforded **2d** as s dark red solid (185 mg, 69%). Mp: 152–153 °C. ^{1}H NMR (400 MHz, DMSO-d_6): δ 8.47 (d, J = 9.2 Hz, 1H), 8.10 (t, J = 8.0 Hz, 2H), 7.99 (t, J = 7.6 Hz, 1H), 7.89 (d, J = 8.0 Hz, 1H), 7.80 (d, J = 9.2 Hz, 1H), 7.73 (t, J = 7.6 Hz, 1H), 7.54 (d, J = 4.0 Hz, 2H), 7.37–7.33 (m, 1H), 7.19 (d, J = 7.6 Hz, 2H), 7.09 (d, J = 7.6 Hz, 2H), 4.16 (s, 2H), 3.94 (s, 3H), 3.22 (s, 3H), 2.23 (s, 3H). ^{13}C NMR (100 MHz, DMSO-d_6): δ 164.1, 158.9, 143.6, 140.4, 139.9, 136.1, 135.7, 133.8, 129.7, 129.6, 128.1, 128.0, 127.5, 126.1, 125.8, 125.5, 124.8, 122.8, 119.2, 114.0, 93.4, 43.1, 41.3, 21.0. HRMS (ESI-TOF) m/z: $[M - I]^+$ calculated for $C_{27}H_{25}N_2S^+$ 409.1733, found 409.1739.

DOI: 10.1021/acs.joc.6b00928
J. Org. Chem. 2016, 81, 6303–6313

*3-Methyl-2-[(1-methyl-2(1H)-quinolinylidene)-p-isopropylbenzylmethyl]benzothiazolium Iodide (**2e**).* According to general procedure B, a mixture of 0.5 mmol of 2TO, 2 mL of *p*-isopropylbenzyl alcohol (**1e**), and 0.15 mmol of $AlCl_3$ was reacted at 110 °C for 6 h under solvent-free conditions. Flash chromatography (methanol/dichloromethane, 1/100 v/v) afforded **2e** as a dark red solid (186 mg, 66%). Mp: 146−147 °C. ^{1}H NMR (400 MHz, DMSO-d_6): δ 8.46 (d, J = 9.2 Hz, 1H), 8.10 (t, J = 8.8 Hz, 2H), 7.99 (t, J = 8.8 Hz, 1H), 7.89 (d, J = 7.8 Hz, 1H), 7.78 (d, J = 9.2 Hz, 1H), 7.72 (t, J = 7.8 Hz, 1H), 7.55 (d, J = 3.6 Hz, 2H), 7.37−7.33 (m, 1H), 7.21 (d, J = 8.0 Hz, 2H), 7.15 (d, J = 8.0 Hz, 2H), 4.17 (s, 2H), 3.94 (s, 3H), 3.24 (s, 3H), 2.85−2.79 (m, 1H), 1.14 (d, J = 6.8 Hz, 6H). ^{13}C NMR (100 MHz, DMSO): δ 164.3, 158.9, 147.1, 143.6, 140.4, 139.9, 136.1, 133.8, 129.6, 128.1, 127.5, 127.1, 126.1, 125.8, 125.6, 124.8, 122.9, 119.1, 114.0, 93.2, 43.2, 41.2, 33.4, 24.3. HRMS (ESI-TOF) m/z: $[M - I]^+$ calculated for $C_{29}H_{29}N_2S^+$ 437.2046, found 437.2058.

*3-Methyl-2-[(1-methyl-2(1H)-quinolinylidene)-p-chlorobenzylmethyl]benzothiazolium Iodide (**2f**).* According to general procedure B, a mixture of 0.5 mmol of 2TO, 10.0 mmol of *p*-chlorobenzyl alcohol (**1f**), and 0.15 mmol of $AlCl_3$ was reacted at 110 °C for 12 h under solvent-free conditions. Flash chromatography (methanol/dichloromethane, 1/50 v/v) afforded **2f** as a dark red solid (117 mg, 42%). Mp: 149−150 °C. ^{1}H NMR (400 MHz, DMSO-d_6): δ 8.50 (d, J = 8.8 Hz, 1H), 8.12 (t, J = 8.0 Hz, 2H), 8.00 (t, J = 7.2 Hz, 1H), 7.89 (d, J = 4.4 Hz, 1H), 7.80 (d, J = 8.8 Hz, 1H), 7.74 (t, J = 7.2 Hz, 1H), 7.54 (d, J = 4.4 Hz, 2H), 7.34 (s, 5H), 4.20 (s, 2H), 3.96 (s, 3H), 3.22 (s, 3H). ^{13}C NMR (100 MHz, DMSO-d_6): δ 164.0, 158.9, 143.6, 140.4, 140.1, 138.0, 133.9, 131.6, 130.2, 129.7, 129.1, 128.1, 127.6, 126.2, 125.8, 125.4, 124.8, 122.9, 119.2, 114.0, 92.6, 43.2, 40.8. HRMS (ESI-TOF) m/z: $[M - I]^+$ calculated for $C_{26}H_{22}ClN_2S^+$ 429.1187, found 429.1202.

*3-Methyl-2-[(1-methyl-4(1H)-quinolinylidene)benzylmethyl]-benzothiazolium Iodide (**3a**).* According to general procedure B, a mixture of 0.5 mmol of 4TO, 2 mL of benzyl alcohol (**1a**), and 0.15 mmol of $AlCl_3$ was reacted at 80 °C for 6 h under solvent-free conditions. Flash chromatography (methanol/dichloromethane, 1/100 v/v) afforded **3a** as a dark purple solid (183 mg, 70%). Mp: 175−176 °C. ^{1}H NMR (400 MHz, DMSO-d_6): δ 8.71 (d, J = 6.8 Hz, 1H), 8.22 (d, J = 8.8 Hz, 1H), 8.02 (t, J = 7.2 Hz, 1H), 7.83 (t, J = 8.0 Hz, 2H), 7.64 (t, J = 7.2 Hz, 1H), 7.58 (d, J = 6.8 Hz, 1H), 7.42 (t, J = 8.8 Hz, 1H), 7.32−7.24 (m, 6H), 7.17 (t, J = 7.2 Hz, 1H), 4.30 (s, 2H), 4.28 (s, 3H), 2.68 (s, 3H). ^{13}C NMR (100 MHz, DMSO-d_6): δ 161.3, 156.7, 145.2, 143.7, 139.5, 134.4, 132.5, 129.1, 128.2, 127.9, 127.4, 127.0, 126.0, 125.3, 124.3, 123.8, 122.7, 119.6, 117.0, 113.1, 109.1, 96.2, 43.7, 43.5. HRMS (ESI-TOF) m/z: $[M - I]^+$ calculated for $C_{26}H_{23}N_2S^+$ 395.1576, found 395.1586.

*3-Methyl-2-[(1-methyl-4(1H)-quinolinylidene)-p-hydroxybenzylmethyl]benzothiazolium Iodide (**3b**).* According to general procedure A, a mixture of 0.5 mmol of 4TO, 2.5 mmol of *p*-hydroxybenzyl alcohol (**1b**), and 0.15 mmol of $AlCl_3$ in 3 mL of anhydrous DMF was reacted at 80 °C for 5 min. Flash chromatography (methanol/dichloromethane, 1/50 v/v) afforded **3b** as a purple solid (167 mg, 62%). Mp: 142−143 °C. ^{1}H NMR (400 MHz, DMSO-d_6): δ 9.26 (s, 1H), 8.71 (d, J = 6.8 Hz, 1H), 8.21 (d, J = 8.4 Hz, 1H), 8.02 (t, J = 8.4 Hz, 1H), 7.82 (d, J = 8.8 Hz, 2H), 7.63 (t, J = 7.2 Hz, 1H), 7.55 (d, J = 6.8 Hz, 1H), 7.41 (t, J = 7.6 Hz, 1H), 7.27 (t, J = 7.6 Hz, 2H), 7.10 (d, J = 8.4 Hz, 2H), 6.64 (d, J = 8.4 Hz, 2H), 4.29 (s, 3H), 4.17 (s, 2H), 2.67 (s, 3H). ^{13}C NMR (100 MHz, DMSO-d_6): δ 161.0, 156.8, 156.4, 145.1, 143.7, 139.1, 134.3, 129.3, 129.2, 128.1, 127.9, 127.4, 126.1, 125.4, 124.2, 122.7, 119.6, 117.0, 115.9, 113.0, 97.1, 43.5, 43.0. HRMS (ESI-TOF) m/z: $[M - I]^+$ calculated for $C_{26}H_{23}N_2OS^+$ 411.1526, found 411.1533.

*3-Methyl-2-[(1-methyl-4(1H)-quinolinylidene)-p-methoxybenzylmethyl]benzothiazolium Iodide (**3c**).* According to general procedure B, a mixture of 0.5 mmol of 4TO, 2 mL of *p*-methoxybenzyl alcohol (**1c**), and 0.15 mmol of $AlCl_3$ was reacted at 80 °C for 0.5 h under solvent-free conditions. Flash chromatography (methanol/dichloromethane, 1/100 v/v) afforded **3c** as a dark purple solid (224 mg, 81%). Mp: 197−198 °C. ^{1}H NMR (400 MHz, DMSO-d_6): δ 8.69 (d, J = 7.2 Hz, 1H), 8.21 (d, J = 8.4 Hz, 1H), 8.02 (t, J = 7.6 Hz, 1H), 7.83 (dd, J = 8.0, 4.0 Hz, 2H), 7.63 (t, J = 7.6 Hz, 1H), 7.56 (d, J = 6.8 Hz, 1H), 7.42 (t, J = 7.6 Hz, 1H), 7.29−7.21 (m, 4H), 6.82 (d, J = 8.4 Hz, 2H), 4.28 (s, 3H), 4.23 (s, 2H), 3.67 (s, 3H), 2.67 (s, 3H). ^{13}C NMR (100 MHz, DMSO-d_6): δ 161.2, 158.3, 156.7, 145.2, 143.7, 139.1, 134.4, 131.1, 129.2, 128.2, 127.9, 127.4, 126.0, 125.3, 124.3, 122.7, 119.6, 117.0, 114.5, 113.1, 96.8, 55.4, 43.5, 42.9. HRMS (ESI-TOF) m/z: $[M - I]^+$ calculated for $C_{27}H_{25}N_2OS^+$ 425.1682, found 425.1689.

*3-Methyl-2-[(1-methyl-4(1H)-quinolinylidene)-p-methylbenzylmethyl]benzothiazolium Iodide (**3d**).* According to general procedure B, a mixture of 0.5 mmol of 4TO, 10.0 mmol of *p*-methylbenzyl alcohol (**1d**), and 0.15 mmol of $AlCl_3$ was reacted at 80 °C for 6 h under solvent-free conditions. Flash chromatography (methanol/dichloromethane, 1/100 v/v) afforded **3d** as a dark purple solid (198 mg, 74%). Mp: 138−139 °C. ^{1}H NMR (400 MHz, DMSO-d_6): δ 8.71 (d, J = 7.2 Hz, 1H), 8.22 (d, J = 8.8 Hz, 1H), 8.02 (t, J = 7.2 Hz, 1H), 7.84−7.81 (m, 2H), 7.63 (t, J = 7.6 Hz, 1H), 7.58 (d, J = 6.8 Hz, 1H), 7.42 (t, J = 7.6 Hz, 1H), 7.28 (d, J = 8.0 Hz, 2H), 7.20 (d, J = 7.6 Hz, 2H), 7.06 (d, J = 8.0 Hz, 2H), 4.28 (s, 3H), 4.25 (s, 2H), 2.67 (s, 3H), 2.21 (s, 3H). ^{13}C NMR (100 MHz, DMSO-d_6): δ 161.2, 156.7, 145.2, 143.7, 139.1, 136.4, 136.0, 134.4, 129.7, 128.2, 128.1, 127.9, 127.4, 126.0, 125.3, 124.3, 122.7, 119.6, 117.0, 113.1, 96.6, 43.5, 43.3, 21.0. HRMS (ESI-TOF) m/z: $[M - I]^+$ calculated for $C_{27}H_{25}N_2S^+$ 409.1733, found 409.1736.

*3-Methyl-2-[(1-methyl-4(1H)-quinolinylidene)-p-isopropylbenzylmethyl]benzothiazolium Iodide (**3e**).* According to general procedure B, a mixture of 0.5 mmol of 4TO, 2 mL of *p*-isopropylbenzyl alcohol (**1e**), and 0.15 mmol of $AlCl_3$ was reacted at 80 °C for 6 h under solvent free conditions. Flash chromatography (methanol/dichloromethane, 1/100 v/v) afforded **3e** as a purple solid (155 mg, 55%). Mp: 136−137 °C. ^{1}H NMR (400 MHz, DMSO-d_6): δ 8.68 (d, J = 6.8 Hz, 1H), 8.21 (d, J = 8.4 Hz, 1H), 8.04−8.00 (m, 1H), 7.84 (t, J = 7.6 Hz, 2H), 7.63 (t, J = 8.0 Hz, 1H), 7.55 (d, J = 6.8 Hz, 1H), 7.42 (t, J = 7.6 Hz, 1H), 7.28 (t, J = 8.4 Hz, 2H), 7.22 (d, J = 8.0 Hz, 2H), 7.14 (d, J = 8.0 Hz, 2H), 4.27 (s, 5H), 2.84−2.77 (m, 1H), 2.68 (s, 3H), 1.13 (d, J = 6.8 Hz, 6H). ^{13}C NMR (100 MHz, DMSO-d_6): δ 166.4, 161.4, 151.7, 149.9, 148.4, 143.9, 141.5, 139.1, 132.9, 132.8, 132.7, 132.2, 131.8, 130.6, 130.2, 129.1, 127.5, 124.4, 121.5, 117.9, 101.1, 48.2, 48.1, 38.1, 29.1. HRMS (ESI-TOF) m/z: $[M - I]^+$ calculated for $C_{29}H_{29}N_2S^+$ 437.2046, found 437.2044.

*3-Methyl-2-[(1-methyl-4(1H)-quinolinylidene)-p-chlorobenzylmethyl]benzothiazolium Iodide (**3f**).* According to general procedure B, a mixture of 0.5 mmol of 4TO, 10.0 mmol of *p*-chlorobenzyl alcohol (**1f**), and 0.15 mmol of $AlCl_3$ was reacted at 80 °C for 12 h under solvent-free conditions. Flash chromatography (methanol/dichloromethane, 1/50 v/v) afforded **3f** as a purple solid (120 mg, 43%). Mp: 107−108 °C. ^{1}H NMR (400 MHz, DMSO-d_6): δ 8.72 (d, J = 6.4 Hz, 1H), 8.22 (d, J = 8.8 Hz, 1H), 8.03 (t, J = 7.6 Hz, 1H), 7.83 (d, J = 8.0 Hz, 2H), 7.64 (t, J = 8.0 Hz, 1H), 7.58 (d, J = 6.4 Hz, 1H), 7.42 (t, J = 7.6 Hz, 1H), 7.36−7.26 (m, 6H), 4.29 (s, 5H), 2.67 (s, 3H). ^{13}C NMR (100 MHz, DMSO-d_6): δ 161.2, 156.6, 145.3, 143.7, 139.1, 138.6, 134.4, 132.5, 131.5, 130.1, 129.1, 128.3, 128.0, 127.4, 126.0, 125.2, 124.3, 123.8, 122.7, 119.7, 117.0, 113.1, 109.0, 95.7, 43.5, 42.9. HRMS (ESI-TOF) m/z: $[M - I]^+$ calculated for $C_{26}H_{22}ClN_2S^+$ 429.1187, found 429.1193.

■ ASSOCIATED CONTENT

Supporting Information

The Supporting Information is available free of charge on the ACS Publications website at DOI: 10.1021/acs.joc.6b00928.

X-ray crystallographic data, ORTEP drawings of the crystal structures, and NMR and HRMS spectra of the products (PDF)

X-ray crystallographic data of 2TO (CIF)

X-ray crystallographic data of 4TO (CIF)

X-ray crystallographic data of **2a** (CIF)

X-ray crystallographic data of **2c** (CIF)

X-ray crystallographic data of **3d** (CIF)

DOI: 10.1021/acs.joc.6b00928
J. Org. Chem. 2016, 81, 6303−6313

AUTHOR INFORMATION

Corresponding Authors

*B.L.: e-mail, libinwhu@nwu.edu.cn.

*L.W.: e-mail, wanglany@nwu.edu.cn; fax, +86 29 81535026.

Notes

The authors declare no competing financial interest.

ACKNOWLEDGMENTS

We appreciate financial support for this research by a grant from the Xi'an Scientific and Technological Plan Projects (CXY1511 (5)), the National Natural Science Foundation of China under Grant Nos. 21575111 and 81201137, and the Natural Science Foundation of Shaanxi Province under Grant No. 2012JC2-10.

REFERENCES

(1) Carreon, J. R.; Stewart, K. M.; Mahon, K. P.; Shin, S.; Kelley, S. O. *Bioorg. Med. Chem. Lett.* **2007**, *17*, 5182.

(2) Mahmood, T.; Paul, A.; Ladame, S. *J. Org. Chem.* **2010**, *75*, 204.

(3) DeLacy, B. G.; Miller, O. D.; Hsu, C. W.; Zander, Z.; Lacey, S.; Yagloski, R.; Fountain, A. W.; Valdes, E.; Anquillare, E.; Soljacic, M.; Johnson; Steven, G.; Joannopoulos, J. D. *Nano Lett.* **2015**, *15*, 2588.

(4) Qin, L.; Xie, F.; Jin, X.; Liu, M. *Chem. - Eur. J.* **2015**, *21*, 11300.

(5) Yoshida, A.; Kometani, N. *J. Phys. Chem. C* **2010**, *114*, 2867.

(6) Deligeorgiev, T.; Kaloyanova, S.; Vasilev, A. *Dyes Pigm.* **2011**, *90*, 170.

(7) Fei, X. N.; Gu, Y. C.; Ban, Y.; Liu, Z. J.; Zhang, B. L. *Bioorg. Med. Chem.* **2009**, *17*, 585.

(8) Carreon, J. R.; Mahon, K. P.; Kelley, S. O. *Org. Lett.* **2004**, *6*, 517.

(9) Bohlaender, P. R.; Wagenknecht, H.-A. *Eur. J. Org. Chem.* **2014**, *2014*, 7547.

(10) Pan, K. Y.; Boulais, E.; Yang, L.; Bathe, M. *Nucleic Acids Res.* **2014**, *42*, 2159.

(11) Fuerstenberg, A.; Julliard, M. D.; Deligeorgiev, T. G.; Gadjev, N. I.; Vasilev, A. A.; Vauthey, E. *J. Am. Chem. Soc.* **2006**, *128*, 7661.

(12) Ohulchanskyy, T. Y.; Pudavar, H. E.; Yarmoluk, S. M.; Yashchuk, V. M.; Bergey, E. J.; Prasad, P. N. *Photochem. Photobiol.* **2003**, *77*, 138.

(13) Jarikote, D. V.; Krebs, N.; Tannert, S.; Roeder, B.; Seitz, O. *Chem. - Eur. J.* **2007**, *13*, 300.

(14) Lau, V.; Heyne, B. *Chem. Commun.* **2010**, *46*, 3595.

(15) Biver, T.; Boggioni, A.; Secco, F.; Turriani, E.; Venturini, M.; Yarmoluk, S. *Arch. Biochem. Biophys.* **2007**, *465*, 90.

(16) Kanony, C.; Akerman, B.; Tuite, E. *J. Am. Chem. Soc.* **2001**, *123*, 7985.

(17) Silva, G. L.; Ediz, V.; Yaron, D.; Armitage, B. A. *J. Am. Chem. Soc.* **2007**, *129*, 5710.

(18) Shank, N. I.; Pham, H. H.; Waggoner, A. S.; Armitage, B. A. *J. Am. Chem. Soc.* **2013**, *135*, 242.

(19) Barrois, S.; Wagenknecht, H.-A. *Org. Biomol. Chem.* **2013**, *11*, 3085.

(20) Stadler, A. L.; Delos Santos, J. O.; Stensrud, E. S.; Dembska, A.; Silva, G. L.; Liu, S. P.; Shank, N. I.; Kunttas-Tatli, E.; Sobers, C. J.; Gramlich, P. M. E.; et al. *Bioconjugate Chem.* **2011**, *22*, 1491.

(21) Karunakaran, V.; Perez-Lustres, J. L.; Zhao, L. J.; Ernsting, N. P.; Seitz, O. *J. Am. Chem. Soc.* **2006**, *128*, 2954.

(22) Wang, S.; Zhang, X. F.; Zhang, J. H.; Bi, W. B.; Wang, L. Y. *RSC Adv.* **2015**, *5*, 64626.

(23) Fu, Y. L.; Huang, W.; Li, C. L.; Wang, L. Y.; Wei, Y. S.; Huang, Y.; Zhang, X. H.; Wen, Z. Y.; Zhang, Z. X. *Dyes Pigm.* **2009**, *82*, 409.

(24) Herz, A. H. *Photogr. Sci. Eng.* **1974**, *18*, 323.

(25) West, W.; Pearce, S. *J. Phys. Chem.* **1965**, *69*, 1894.

(26) McNamara, L. E.; Liyanage, N.; Peddapuram, A.; Murphy, J. S.; Delcamp, J. H.; Hammer, N. I. *J. Org. Chem.* **2016**, *81*, 32.

(27) Zhang, S.; Fan, J. l.; Li, Z. Y.; Hao, N. J.; Cao, J. F.; Wu, T.; Wang, J. Y.; Peng, X. J. *J. Mater. Chem. B* **2014**, *2*, 2688.

(28) Shank, N. I.; Zanotti, K. J.; Lanni, F.; Berget, P. B.; Armi-tage, B. A. *J. Am. Chem. Soc.* **2009**, *131*, 12960.

(29) Toutchkine, A.; Nguyen, D.; Hahn, K. M. *Org. Lett.* **2007**, *9*, 2775.

(30) Aubry, J. M. *J. Am. Chem. Soc.* **1985**, *107*, 5844.

(31) Boehme, K.; Brauer, H. D. *Inorg. Chem.* **1992**, *31*, 3468.

(32) Reed, A. E.; Curtiss, L. A.; Weinhold, F. *Chem. Rev.* **1988**, *88*, 899.

(33) Brooker, L. G. S.; Keyes, G. H.; Williams, W. W. *J. Am. Chem. Soc.* **1942**, *64*, 199.

(34) Mejia-Garcia, T. A.; Paes-de-Carvalho, R. *J. Neurochem.* **2007**, *100*, 382.

DOI: 10.1021/acs.joc.6b00928
J. Org. Chem. 2016, 81, 6303−6313